Available online at www.sciencedirect.com
ScienceDirect
Journal of Power Sources 160 (2006) 187–193
JOURNAL OF POWER SOURCES
www.elsevier.com/locate/jpowsour

Review

Ultrasonically treated multi-walled carbon nanotubes (MWCNTs) as PtRu catalyst supports for methanol electrooxidation

Chunwei Yang [a,*], Xinguo Hu [a], Dianlong Wang [a], Changsong Dai [a], Liang Zhang [b], Haibo Jin [b], Simeon Agathopoulos [c]

[a] *Department of Applied Chemistry, Harbin Institute of Technology, Harbin 150001, PR China*
[b] *School of Materials Science and Engineering, Beijing Institute of Technology, Beijing 100081, PR China*
[c] *Department of Materials Science and Engineering, University of Ioannina, GR-451 10 Ioannina, Greece*

Received 2 April 2006; received in revised form 2 May 2006; accepted 3 May 2006
Available online 11 July 2006

Abstract

In the quest of fabricating supported catalysts, experimental results of transmission electron microscopy, Raman and infrared spectroscopy indicate that ultrasonic treatment effectively functionalizes multi-walled carbon nanotubes (MWCNTs), endowing them with groups that can act as nucleation sites which can favor well-dispersed depositions of PtRu clusters on their surface. Ultrasonic treatment seems to be superior than functionalization via regular refluxing. This is confirmed by the determination of the electrochemistry active surface area (ECA) and the CO-tolerance performance of the PtRu catalysts, measured by adsorbed CO-stripping voltammetry in 0.5 M sulfuric acid solution, and the real surface area of the PtRu catalysts, evaluated by Brunauer–Emmett–Teller (BET) measurements. Finally, the effectiveness for methanol oxidation is assessed by cyclic voltammetry (CV) in a sulfuric acid and methanol electrolyte.

Keywords: Carbon nanotubes; Surface treatment; Raman spectroscopy; Functional groups; Catalyst supports; DMFC

Contents

1. Introduction

Direct methanol fuel cells (DMFCs) are being intensively investigated because of their potential as clean and mobile sources of power [1]. PtRu is the most active anode alloy catalyst for DMFCs [2]. The PtRu catalysts are usually dispersed on high surface area carbon supports, such as carbon nanotubes [3,4]. Beyond catalysis, multi-walled carbon nanotubes (MWCNTs) have attracted great interest because of their remarkable electrical, mechanical, and structural properties.

To deposit catalytic metal nanoparticles with a high loading onto MWCNTs, surface functionalization is necessary. Among

* Corresponding author. Tel.: +86 451 86413751; fax: +86 451 86412750.
E-mail address: cw.yang@hit.edu.cn (C. Yang).

0378-7753/$ – see front matter © 2006 Elsevier B.V. All rights reserved.
doi:10.1016/j.jpowsour.2006.05.015

various methods of functionalization, surface oxidation is probably the most widely studied, because amorphous carbon can be removed from the non-activated MWCNTs [5]. Furthermore, it favors the opening of the MWCNT ends and thus the insertion of metal nanoparticles [6]. Earlier results have indicated that activated MWCNT supports provide a higher catalytic activity than non-activated MWCNTs supports. Nevertheless, the reason for this difference still remains unclear. Liquid-phase oxidation, which involves the use of nitric and/or sulfuric acids, is mild and slow, and can provide a high yield of oxidized MWCNTs, compared to gas-phase oxidation.

Several papers deal with the application of carbon nanotubes in fuel cells as catalyst supports and as electrode materials [7–11]. Wu et al. [12] have shown that Pt nanoparticles supported on carbon nanotubes produce a much higher maximum power density than those supported on carbon black in DMFCs. Many studies have focused on the chemical modifications of MWCNTs to improve the dispersion of metal particles. However, the dispersion of metals on MWCNTs by chemical methods is largely based on conventional catalyst preparation techniques, such as wet impregnation followed by reduction [13].

This study aims to compare ultrasonic and refluxing treating methods of MWCNTs, with regards to the resulting surface structure and electrochemical characteristics. The surface functional groups and the structure of MWCNTs were determined with the aid of Raman, infrared spectroscopy and transmission electron microscopy (TEM).

2. Materials and experimental procedure

2.1. Preparation of materials

MWCNTs, with purity of 95% and a diameter of 30 nm, synthesized by chemical vapor deposition, were immersed in an acidic mixture of 69% HNO_3 and 98% H_2SO_4 solutions (mass ratio 2/3).

For the ultrasonic treatment, an ultrasonic probe, covered with PTFE (for protection from the acids), was placed into the mixture. The treatment, carried out at room temperature, lasted 2 h. The ultrasonic frequency was 25 kHz. For the reflux-treatment, the MWCNTs and the solution of the two acids were put together in a flask with three openings, churned for 5 min and refluxed for 24 h. The treated MWCNTs were centrifugally separated from the acids, and then thoroughly washed with deionized water.

A colloidal method was employed to produce the carbon nanotubes for the PtRu catalyst, according to the description of Watanabe et al. [14]. Complexes of Pt sulfite and Ru sulfite were synthesized in aqueous solution. Addition of hydrogen peroxide caused oxidation and decomposition, simultaneously with adsorption onto the activated MWCNTs, already suspended in the solution. After washing with water, the catalysts were reduced in a flowing stream of hydrogen at 300 °C. The Pt/Ru ratio was 1/1 and the metal loading 20% (by weight). Three different catalysts were produced, denoted as PtRu/MWCNTs for the non-activated support, PtRu/R-MWCNTs for the reflux activation, and PtRu/S-MWCNTs for the ultrasonic activation.

2.2. Characterization

Transmission electron microscopy (TEM) was employed to observe the morphology of the catalysts (TEM Philips, operated at 300 kV), using 400-mesh carbon-coated copper TEM grids (Electron Microcopy Sciences, CF-400Cu). The samples were also analyzed by Raman (co-focus laser Raman spectroscopy apparatus LabRam Infinity, JY Company; Ar^+ laser emitter with wavelength at 514.5 nm; resolution 1 cm^{-1}) and infrared spectroscopy (Perkin-Elmer 2000 FT-IR spectrometer, equipped with a diffusion reflectance detector to measure the diffusion reflectance infrared Fourier transform, DRIFT, spectra). The BET surface areas of the catalyst samples were measured by N_2 adsorption using a Micromeritics ASAP2010 apparatus.

Electrochemical measurements were conducted at room temperature in a three-compartment electrochemical cell. A carbon paper, pasted with The PtRu/MWCNTs catalysts, was used as the working electrode. A Pt-gauze and a saturated calomel electrode (SCE) were used as counter and reference electrodes, respectively. All potentials reported in this paper are with respect to RHE. An EG&G model 273 potentiostat/galvanostat was used. The electrochemical active surface area (ECA) was assessed using CO-stripping techniques. CO was adsorbed onto the working electrode surface by bubbling high-purity CO through the 0.5 M H_2SO_4 electrolyte bathing the electrode for 12 h while holding the potential at 30 mV versus RHE. After the adsorption, the dissolved CO was removed from the solution by bubbling high-purity argon for 30 min while still holding the potential at 30 mV. The potential was then scanned in a positive direction from 0 mV versus RHE at 20 mV s^{-1}. For methanol electrooxidation, CV were carried out in a solution of 2 M CH_3OH/0.5 M H_2SO_4. Prior to electrochemical measurements, the electrolyte solutions were purged with high-purity argon for 30 min.

3. Results and discussion

3.1. Surface oxidation of the MWCNTs

Fig. 1 shows typical TEM images of the MWCNTs. A stacking together of many carbon nanoparticles and other impurities of carbon origin characterize the non-activated MWCNTs (Fig. 1(a)). The reflux (Fig. 1(b)) and the ultrasonic treatments (Fig. 1(c)) both caused an increase of the isolation of the MWCNTs, while nearly no carbon nanoparticle agglomerations were observed. The acidic etching should cause the observed roughening of the surface of the MWCNTs, which is more evident in the case of the ultrasonic treatment. In this case (Fig. 1(c)), the MWCNTs seem to be shorter, while the tubes are abundantly opened. Hence, the metal can easily deposit at the mouth and at any coarsened locations on the nanotubes (for energetic reasons).

Ultrasonic treatment also caused a thinning of the walls of the nanotubes (Fig. 1(e), comparing to Fig. 1(d) for reflux treatment). Evidently, in the ultrasonic field, the MWCNTs are quickly vibrated in the acidic solution, and they split apart, while carbon nanoparticles fall from the nanotubes. Cavitation

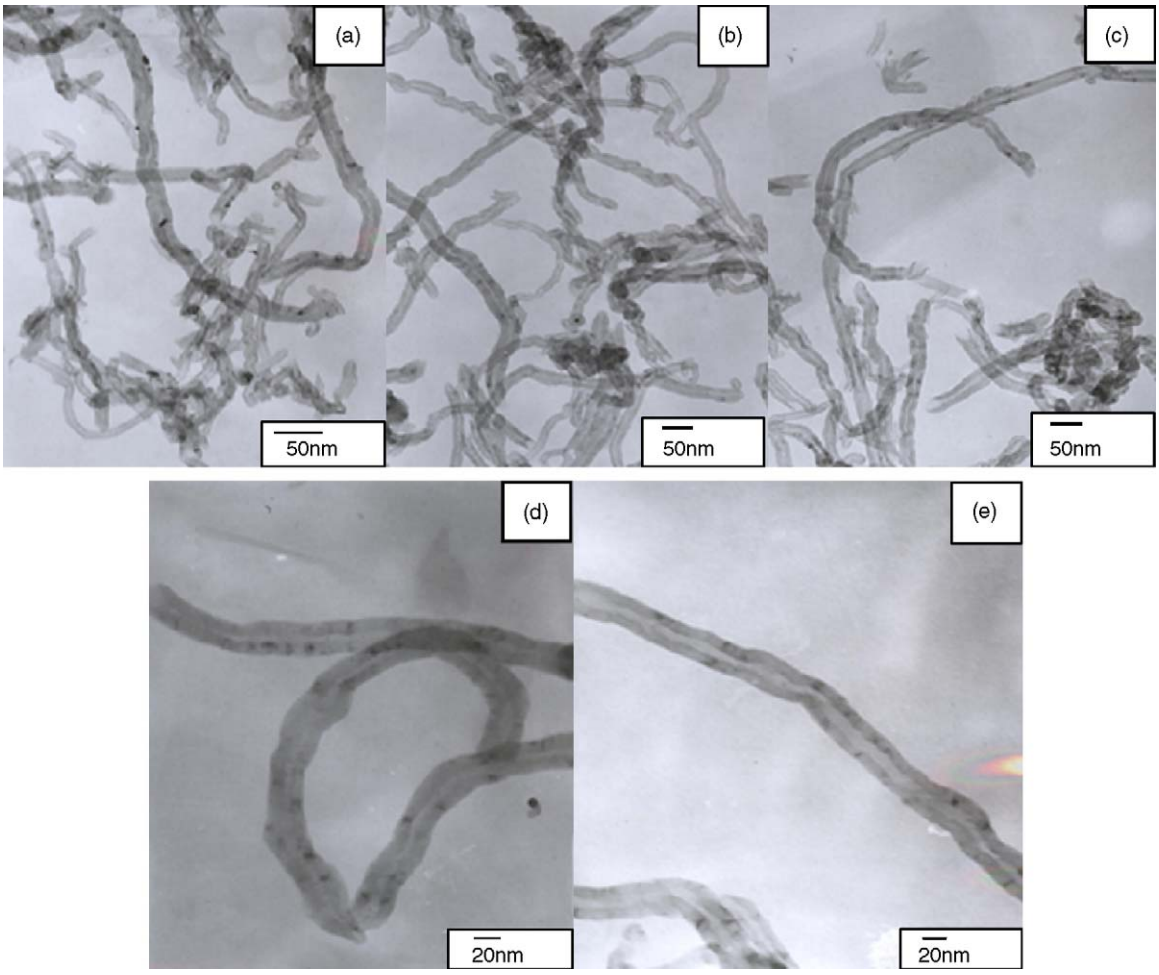

Fig. 1. TEM images of (a) non-treated MWCNTs, (b) R-MWCNTs, (c) S-MWCNTs, (d) R-MWCNTs, and (e) S-MWCNTs.

could also play an important role in the ultrasound treatment. High temperature, high pressure, and shock waves, generated by the prompt breaking of gas cavities, could cause opening of MWCNT tubes and shortening of their lengths [15]. At the same time, the surface functional groups should uniformly be build up on the tube walls. Consequently, ultrasonic treatment can be considered as an effective method to functionalize the MWCNT surface, taking into account the short time needed (2 h), comparing to the reflux treatment.

Fig. 2 shows the effect of surface treatment on the Raman spectrum of the raw MWCNTs. Three principal bands and a weak band are generally observed between 1000 and 3500 cm^{-1}. The band with a maximum at ~1348 cm^{-1} is common for disordered sp^2 carbon and has been called the D-band. The band which peaked at ~1580 cm^{-1} is close to that observed for well-ordered graphite, and it is often called as G-band or E_{2g} band. The vibrational mode of C–H, usually resulting in a band at 2912 cm^{-1}, is indicative of the hydrogen produced during oxidation.

The intensity ratio between the D-band (I_D) and the G-band (I_G) is sensitive to the chemical processing. Hence, the value of the I_D/I_G ratio is an index of graphitization degree of MWCNTs due to oxidation. For the non-activated MWCNTs, the I_D/I_G ratio was calculated as 1.076, indicating a great amount of amorphous carbon or existance of defects on the surface of the nanotubes.

After ultrasonic treatment, the I_D/I_G ratio increased to 1.100. Taking into account the results of the TEM observations (Fig. 1(c) and (e)), which have shown that there is no amorphous carbon and impurities on the surface of the ultrasonically treated MWCNTs, the higher I_D value may be due to defects on

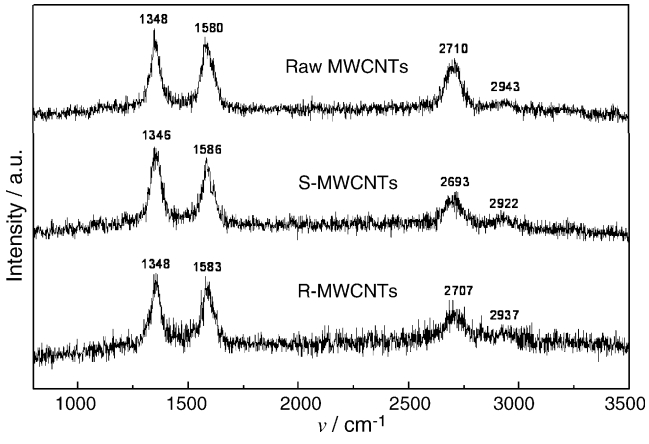

Fig. 2. Raman spectra of non-treated MWCNTs, R-MWCNTs and S-MWCNTs.

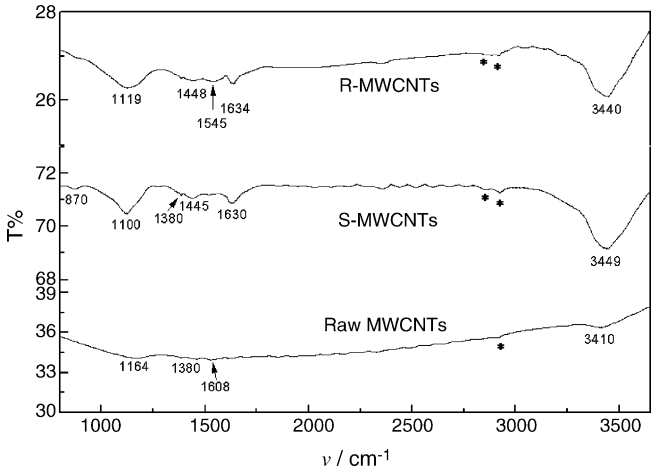

Fig. 3. FT-IR spectra of non-treated MWCNTs, R-MWCNTs and S-MWCNTs.

the surface of the nanotubes. Bacsa et al. [16] have reported that the graphite arrangement of perfect MWCNTs generates a helical structure, which makes the accumulation of adjacent graphite deviate from the typical hexagonal configuration. To decrease this deviation and the total energy of the system, MWCNTs usually adjust their microstructure in such as a way as to reduce the stress in the graphite layers by their defects. It is well-known that cavitation bubbles, produced in liquid solution during sonication, can instantaneously generate local spots with very high temperature, reaching several thousand degrees, and a very high pressure, of several thousand atmospheres [17]. Hence, with the ultrasonic treatment, the weak bonds begin to break and the oxygen-containing groups are modified on the surface of the MWCNTs.

The I_D/I_G ratio of the MWCNTs treated by reflux was calculated as 1.028, suggesting a small number of defects on the surface. A red shift of the G-band peak of the oxidized specimen was observed. Hiura et al. [18] have assigned the softening of the G-band to the quanta effect and the diameter distribution of the MWCNTs.

The FT-IR spectra of activated and non-activated MWCNTs are plotted in Fig. 3. Table 1 summarizes the assignment of the main bands observed to the functional groups. A peak at $\sim$2900 cm^{-1} (marked by asterisks) can be assigned to the C–H_n functional groups or to the C–H stretching mode of the functionalized alkyl chains in the MWCNTs [19]. A broad band at $\sim$3400 cm^{-1} is assigned to a variety of O–H stretching modes. The wide width of this band suggests that several different –OH groups are probably present in many different chemical environments [20]. Carboxylic acid groups are likely indicated by the C=O band at $\sim$1600 cm^{-1}. The band at 1100 cm^{-1} is located in the range of C–O stretching modes of ethers, esters, alcohols, and phenol compounds. The intensity of the peak indicates changes of the dipole moment that is bigger with increasing polarity of the group [21].

In general, the FT-IR spectra suggest that the surface of the MWCNTs is prone to absorb many hydroxyl and carbonyl groups. From a comparison of the plots of the S-MWCNTs and R-MWCNTs, it seems that in the former, many polar groups are generated on the nanotubes than after the reflux treatment.

3.2. TEM analysis of the PtRu/MWCNTs catalysts

The dispersion of PtRu spherical clusters on activated MWCNTs, shown in Fig. 4, was high and uniform, featuring a narrow particle size distribution, in particular between 4 and 10 nm for the reflux treatment (Fig. 4(a)) and 2–4 nm for the ultrasonic treatment (Fig. 4(b)). These results are due to the large number of oxygen-containing groups on the surface. The high metal deposition on the openings of the nanotubes is due to the hanging-bonds produced there. Yoshio et al. [22] have reported that the PtRu particles with ca. 3.0 nm in size exhibit the highest-mass catalytic activity for methanol electrooxidation.

3.3. Evaluation of EAS and CO-tolerant performance of the PtRu/MWCNTs catalysts

Fig. 5 shows the base voltammogram (dashed line) and CO-stripping (solid line) on the PtRu catalysts at 20 mV s^{-1} in 0.5 M H_2SO_4 electrolyte. It should be noted that the adsorbed CO has been oxidized completely in a single scan and no CO_{ads} oxidation is monitored during the second scan for all the three catalysts. For the sake of clarity, only the first cycle is shown in Fig. 5. For comparison, In the high potential range, in which the oxidation is usually attributed to the linear-bonded CO_{ads} [23], the PtRu/S-MWCNTs nanocomposite has a peak potential of 0.59 V, which is 100 and 350 mV lower than the PtRu/R-MWCNTs (0.71 V) and the PtRu/MWCNTs (0.89 V), respectively. Consequently, the ultrasonically treated MWCNTs as supports for the PtRu catalysts have an excellent CO-tolerant performance.

The ECA can reflect the intrinsic electrocatalytic activity of a catalyst. The ECA of the PtRu/S-MWCNTs, the PtRu/R-MWCNTs and the PtRu/MWCNTs catalysts are listed in Table 2. Evidently, the ECA of the PtRu/S-MWCNTs catalysts is much higher than the other two investigated catalysts. This may be due to the high dispersion of PtRu on the function-

Table 1
Assignment of IR bands observed in the spectra of different MWCNTs

Frequency (cm^{-1})	Support	Assignment
$\sim$1100	R-MWCNTs, S-MWCNTs, raw MWCNTs	C–O stretching in ethers, esters, alcohol, and phenol compounds
$\sim$1380	Raw MWCNTs, S-MWCNTs	Interactions between O–H bending and C–O stretching in phenol group
$\sim$1440	Raw MWCNTs	Conjugation of C=O with C=C bonds or interactions between localized
$\sim$1600	R-MWCNTs, S-MWCNTs, raw MWCNTs	C=C bonds and carboxylic acids and ketones
$\sim$3400	R-MWCNTs, S-MWCNTs, raw MWCNTs	O–H stretching in alcoholic or phenolic groups

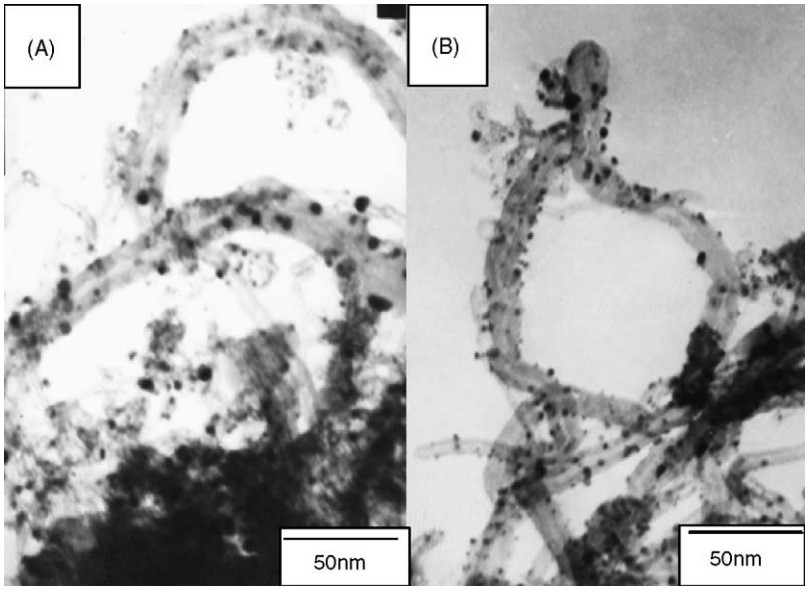

Fig. 4. TEM images of (a) PtRu/R-MWCNTs and (b) PtRu/S-MWCNTs catalysts.

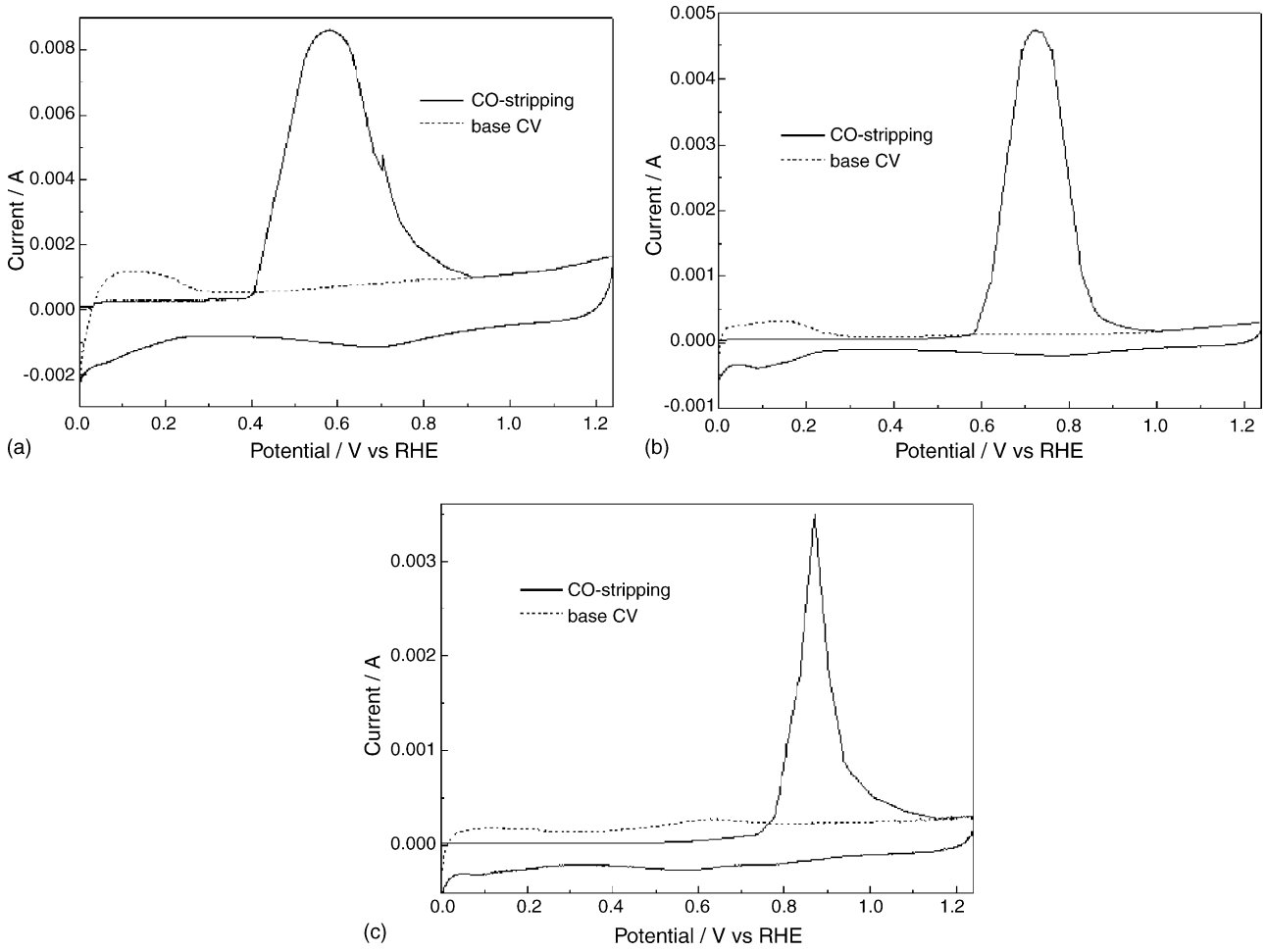

Fig. 5. CO-stripping voltammograms of (a) PtRu/S-MWCNTs, (b) PtRu/R-MWCNTs, and (c) PtRu/MWCNTs catalysts in 0.5 M H_2SO_4 at 25 °C; scanning rate, 20 mV s^{-1}.

Table 2
BET surface area and ECA of the PtRu catalysts

Catalyst	BET surface area ($m^2\ g^{-1}$ metal)	ECA ($m^2\ g^{-1}$ metal)
PtRu/S-MWCNTs	116	97.9
PtRu/R-MWCNTs	103	55.7
PtRu/MWCNTs	92	30.3

alized surface of the MWCNTs and the creation of new active sites for PtRu.

Obviously, the ECA of the PtRu catalysts is different from the total particle surface area as calculated, e.g. from the metal loading and the dispersion or from the BET measurements. It was lower than the surface area found in the N_2 BET measurements (Table 2). This result can be rationalized assuming that part of the metal particle surface is covered by RuO_2 and/or PtO [24]. This effect leads to a reduction of the accessible chemically-active noble metal, since adsorption of CO takes place exclusively on oxide-free noble metal surface sites.

Table 2 also compares the catalysts real surface areas as determined from BET. It can be seen that the PtRu/S-MWCNTs catalysts have a larger real surface area. This indicated that the PtRu metals can better disperse on the surface of MWCNTs treated ultrasonically. This result is due to the large number of oxygen-containing groups on the surface.

3.4. Methanol electrooxidation of the PtRu/MWCNTs catalysts

After having characterized the different surface areas of the PtRu catalysts by CO-stripping and BET, we now focus on their activity for the oxidation of methanol. The methanol oxidation activity of the three investigated the PtRu catalysts was evaluated by the CV plots shown in Fig. 6. Evidently, the oxidation activity of the PtRu/S-MWCNTs catalysts is much higher than the other catalysts, which agrees fairly well with reference [25]. A low activity for methanol electrooxidation was observed for the PtRu/R-MWCNTs catalysts, likely due to the formation of aggregations, whereby Ru particles may overlay Pt. In that case, methanol cannot be adsorbed onto the surface of the catalyst, and thus it cannot be electrochemically reduced during methanol oxidation. This conclusion agrees fairly well with the CO-stripping results mentioned above.

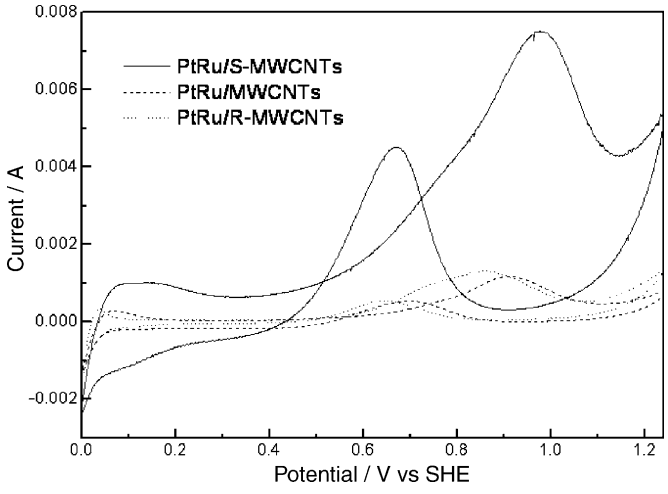

Fig. 6. Cyclic voltammetry of PtRu/S-MWCNTs, PtRu/R-MWCNTs, and PtRu/MWCNTs catalysts in 2 M CH_3OH/0.5 M H_2SO_4 electrolyte at 25 °C; scanning rate, 50 mV s^{-1}.

4. Conclusion

This study investigated two pretreatment methods for multiwalled carbon nanotubes (MWCNTs), which were produced to support PtRu nanoparticle catalysts for methanol electrooxidation. The characterizations made by TEM and IR and Raman spectroscopy revealed that the MWCNTs activated by ultrasonic treatment exhibited a more uniform surface, shorter length, higher separation, openings and modified surfaces with oxygen-bearing functional groups, which favors PtRu loading. CO-stripping voltammetry afforded an approximate evaluation of the ECA and the CO-tolerance of the PtRu catalysts, showing that the PtRu/S-MWCNTs catalysts had the highest ECA and the best CO-tolerance. The superiority of the PtRu/S-MWCNTs catalysts was also confirmed by the analysis of the results using CV, with regard to the catalytic activity in the electrooxidation of methanol. This was attributed to the better dispersion and utilization of the PtRu particles on the surface of the MWCNTs, modified with oxygen-bearing functional groups ultrasonically.

References

[1] R. Dillon, S. Srinivasan, A.S. Arico, V. Antonucci, International activities in DMFC R&D: status of technologies and potential applications, J. Power Sources 127 (1–2) (2004) 112–126.
[2] B. McNicol, D. Rand, K. Williams, Direct methanol–air fuel cells for road transportation, J. Power Sources 83 (1/2) (1999) 15–31.
[3] Y. Liang, H. Zhang, B. Yi, Z. Zhang, Z. Tan, Preparation and characterization of multi-walled carbon nanotubes supported. The PtRu catalysts for proton exchange membrane fuel cells, Carbon 43 (15) (2005) 3144–3152.
[4] L.D. Bruke, M.A. Horgan, L.M. Hurley, L.C. Nagle, A.P. Mullane, Superactivation of metal electrode surfaces and its relevance to CO_{ads} oxidation at fuel cells anodes, J. Appl. Electrochem. 31 (2001) 729–738.
[5] T.W. Ebbesen, Decoration of carbon nanotubes, Adv. Mater. 8 (2) (1996) 155–162.
[6] T.W. Ebbesen, P.M. Ajayan, H. Hiura, K. Tanigaki, Purification of nanotubes, Nature 367 (6463) (1994) 519.
[7] H. Wang, T. Loffler, H. Baltruschat, Formation of intermediates during methanol oxidation: a quantitative DEMS study, J. Appl. Electrochem. 31 (2001) 759–765.
[8] T. Matsumoto, T. Komatsu, H. Nakano, K. Arai, Y. Nagashima, E. Yoo, et al., Efficient usage of highly dispersed Pt on carbon nanotubes for electrode catalyst of polymer electrolyte fuel cells, Catal. Today 90 (2004) 277–281.
[9] W. Li, C. Liang, J. Qiu, W. Zhou, H. Han, Z. Wei, et al., Carbon nanotubes as support for cathode catalyst of a direct methanol fuel cell, Carbon 40 (2002) 703–787.
[10] G.G. Kumar, M. Rettker, R. Underhile, D. Binc, K. Vinodgopal, P. McGinn, Single-wall carbon nanotube-based proton exchange membrane assembly for hydrogen fuel cells, Langmuir 21 (2005) 8487–8494.
[11] W. Li, C. Liang, W. Zhou, J. Qiu, Z. Zhou, G. Sun, et al., Preparation characterization of multiwalled carbon nanotube-supported platinum for cathode catalysts of direct methanol fuel cells, J. Phys. Chem. B 107 (2003) 6292–6299.

[12] G. Wu, Y.S. Chen, B.Q. Xu, Remarkable support effect of SWNTs in Pt catalyst for methanol electrooxidation, Electrochem. Commun. 7 (2005) 1237–1243.
[13] B. Xue, P. Chen, Q. Hong, J.Y. Lin, K.L. Tan, Growth of Pd, Pt, Ag and Au nanoparticles on carbon nanotubes, J. Mater. Chem. 11 (9) (2001) 2379–2382.
[14] M. Watanabe, M. Uchida, S. Motoo, Preparation of highly dispersed Pt + Ru alloy clusters and the activity for the electrooxidation of methanol, J. Electroanal. Chem. 229 (1/2) (1987) 395–406.
[15] K.L. Lu, R.M. Lago, Y.K. Chen, M.L.H. Green, P.J.F. Harris, S.C. Tsang, Mechanical damage of carbon nanotubes by ultrasound, Carbon 34 (6) (1996) 814–816.
[16] W.S. Bacsa, D. Ugarte, A. Chatelain, W.A. de Heer, High-resolution electron microscopy and inelastic light scattering of purified multishelled carbon nanotubes, Phys. Rev. B 50 (20) (1994) 15473–15476.
[17] K.S. Suslick, Application of ultrasound to materials chemistry, MRS Bull. 20 (4) (1995) 29–34.
[18] H. Hiura, T.W. Ebbesen, K. Tanigak, Raman studies of carbon nanotubes, Chem. Phys. Lett. 202 (6) (1993) 509–512.
[19] M.A. Hamon, P. Bhowmik, H. Hu, S. Nivogi, B. Zhao, M.E. Itkis, R.C. Haddon, End-group and defect analysis of soluble single-walled carbon nanotubes, Chem. Phys. Lett. 347 (1–3) (2001) 8–12.
[20] K. Un Jeong, A.F. Clascidia, L. Xiaoming, C. Gugang, C.E. Peter, Raman and IR Spectroscopy of chemically processed single-walled carbon nanotubes, J. Am. Chem. Soc. 127 (2005) 15437–15445.
[21] C. Jie, S. Qize, Organic Spectroscopy Analysis, Beijing Institute of Technology Press, PR Beijing, 1996, p. 48.
[22] T. Yoshio, I.T. Hiroyuki, I. Tomoya, M. Ryo, O. Takefumi, S. Wataru, et al., Size effects of ultrafine Pt–Ru particles on the electrocatalytic oxidation of methanol, Chem. Commun. 1 (4) (2001) 341–342.
[23] L. Jiang, G. Sun, X. Zhao, Z. Zhou, S. Yan, S. Tang, et al., Preparation pf supported The PtRu/C electrocatalyst for direct methanol fuel cells, Electrochim. Acta (50) (2005) 2371–2376.
[24] Z. Jusys, T.J. Schmidt, L. Dubau, K. Lasch, L. Jörissen, J. Garche, et al., Activity of the $PtRuMeO_x$ (Me = W, Mo or V) catalysts towards methanol oxidation and their characterization, J. Power Sources (105) (2002) 297–304.
[25] C.X. Yang, Synthesis and electrochemical characterization of uniformly-dispersed high loading Pt nanoparticles on sonochemically-treated carbon nanotubes, J. Phys. Chem. B 108 (50) (2004) 19255–19259.